4th International Conference on Inventive Research in Computing Applications (ICIRCA 2022)

21-23, September 2022 | Coimbatore, India

Proceedings

IEEE XPLORE COMPLIANT ISBN: 978-1-6654-9707-7
IEEE DVD ISBN: 978-1-6654-9706-0

organized by

RVS College of Engineering & Technology

Coimbatore, Tamil Nadu, India

2022 4th International Conference on Inventive Research in Computing Applications (ICIRCA) | 978-1-6654-9707-7/22/$31.00 ©2022 IEEE | DOI: 10.1109/ICIRCA54612.2022.9985616

2022 4th International Conference on Inventive Research in Computing Applications (ICIRCA) | 978-1-6654-9707-7/22/$31.00 ©2022 IEEE | DOI: 10.1109/ICIRCA54612.2022.9985545

4th International Conference on Inventive Research in Computing Applications (ICIRCA 2022)

21-23, September 2022

Table of Contents

Detecting Space Debris using Deep Learning Algorithms: A Survey

Piyush Jharbade
Department of Computer Science Engineering
Madhav Institute of Technology and Science
Gwalior, India
PiyushJharbade@ieee.org

Manish Dixit
Department of Computer Science Engineering
Madhav Institute of Technology and Science
Gwalior, India
ManishDixit@ieee.org

2022 4th International Conference on Inventive Research in Computing Applications (ICIRCA) | 978-1-6654-9707-7/22/$31.00 ©2022 IEEE | DOI: 10.1109/ICIRCA54612.2022.9985622

Abstract- A collection of natural micrometeoroids and artificial items orbiting the earth is known as space debris. Artificial space debris consists of non-operational satellites, parts of rocket, and junk ejected by the spacecrafts etc. Kessler Syndrome dictates that the danger of space debris could be accelerated by collisions among them which will cause a chain reaction that will result in uninhabited earth orbit and leading to the growth of a belt of debris around the earth. The substantial rise in the total quantity of space debris in Earth's orbit poses a severe risk to active spacecraft and satellites. Impacts of orbital space debris on satellites, spacecrafts and huge space assets are serious risk that can seriously affect mission success. Therefore, space debris detection is crucial for satellite protection and space disaster prevention. Furthermore, space debris identification is complex due to its rapid relative velocity and distortions caused by solar radiation in orbit-based monitoring systems. Moreover, space based known objects can be tracked with a telescope from here on earth, while unknown objects cannot. Vision sensors such as monocular photographic cameras are considered as a major job for the detection of space debris, however, these tasks are difficult due to a semantic division between observable characteristics of space debris, as well as a lack of measurable and credible visual information in space environment. Various strategies are available for detecting space debris. However, image-based space debris detection algorithms inspired by powerful pattern recognition ability of deep convolutional neural networks (DCNN) have been examined in this survey and a comprehensive analysis is carried out to define the research issues and progress in this domain.

Keywords: Space debris, Lightcurve, Deep learning(DL), Deep convolutional neural network (DCNN), Machine learning.

I. INTRODUCTION

A collection of natural micrometeoroids and artificial items orbiting the earth is known as space debris. [1] Any man-made object orbiting the Earth that no longer serves a useful function is a space debris, artificial space debris consists of non-functional satellites, rocket bodies, and junk ejected by the spacecrafts etc. [2]. Debris can also develop in orbit as a result of debris colliding with satellites or debris colliding with debris, with the increase in human exploration to the outer-space a new problem known as space debris problem has emerged. Countless, hard to track and dangerous are some of the key reasons why space debris is a potential threat to the safety of space assets [3]. A typical classification of space debris is shown in Table 1.

TABLE I. CLASSIFICATION AND CHARACTERISTICS OF SPACE DEBRIS

Type	Orbital Speed(mph)	Size(meter)	Remarks
Nonfunctional spacecraft	up to 15,000 mph	> 5m	Can be tracked by network of telescopes.
Abandoned launch vehicle stages	up to 15,000 mph	> 10m	Can be tracked by network of telescopes.
Fragmentation debris	up to 17,500 mph	< 0.001m	Very hard to detect, track and lacks visual features.
Mission-related debris	up to 15,000 mph	<0.1m	Hard to track

Over the past years, space debris has become a major problem to astronomers and space operators, estimated by the European space agency there are over 130 million pieces of space debris with the diameter of less than 1cm, 1 million with the diameter between 1-10 cm and 36,500 pieces of space debris with the diameter greater than 10 cm [4], most of them travelling at over 15,700 miles per hour [5], therefore even the smallest debris could cause a catastrophe in space and its prevention is necessary for the success of future space missions [6]. A structured solution for space debris problem is shown in a 3-step process in Figure. 1 viz. Prevention, Capture/Identification and Removal. In this paper we are going to focus on the identification aspect of space debris.

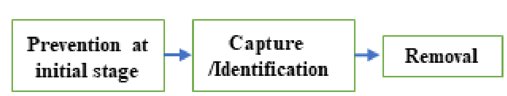

Fig. 1. Model representation of the 3-step solution

To identify any space-based target, we need an observer that can make observations in in-situ, remote, or both situation, and ground tests are performed to help analyze those results [7]. In this paper our focus will be on in-situ or space-based observers. Space-based observers are essential for various image processing tasks carried out with respective to deep space images, orbit-based images as well as satellite images of earth. Satellite-based space images are used for - autonomous navigation for deep space exploration [8], exploring exoplanets in distant galaxies [9], detecting distant galaxies [10] and detecting objects in earth's orbit. Satellite images of earth are used in identifying agriculture fields [11].

An space-based observer for debris detection is a dedicated small satellite with a space debris sensor payload – such as a 3D-mapping lidar system, a cascade detecting system of millimeter-wave radar embedded with optical lidar sensor, or a newly-developed multispectral sensor allowing for debris items characterization, the observer is launched into a dedicated lower earth orbit ideal for space debris detection [12], the sensor payload record the items per unit of time as they move across a small but well-defined region of space and the sensor calibration is then tested by comparing the observed flux to the flux that is computed from the orbital telemetry data of objects in various space debris catalogs like United States Strategic Command (USSTRATCOM) catalog for space debris [13].

There are variety of approaches available for the identification, estimating parameters, determining attributes and location of the space debris [14] [15]. However, the majority of them are derived from artificial characteristics, and their accuracy is hindered by adverse space conditions [16].

Features with notable characteristics can be obtained for objects, thanks to the advancement of deep learning networks [17]. AlexNet [18] initially processed data using 5 convolutional layers, indicating that deep learning networks can outperform various conventional classification techniques. Then the advancement in network architecture became deeper with the development of VGGNet [19], GoogleNet [20], ResNet [21]. A deeper network in the domains of image analysis, segmentation, and localization indicates that more information can be retrieved. As a result, it boosts the performance. In contrast to the broad approaches of convolutional neural networks (CNNs) for detecting and recognising ground-based images, space objectives are still handled using the manual interpretation technique [22]. However, various traditional automatic feature extraction techniques for space debris identification exists, but their applications are confined to short distance space debris classifications and not for deep space targets. Moreover, these approaches are incapable of real-time processing and these inabilities can be accomplished by employing DL techniques to identify and characterise space debris. This paper shows that deep learning algorithms of CNNs can be used to recognize space debris [23].

Sections arranged in rest of the paper are as follows, Section II discusses various identification techniques for space debris. Section III examines the strategies for identifying space debris using CNN in a tabular style, followed by conclusion in Section IV.

II. LITERATURE SURVEY

The two major methodologies used to detect and classify space debris are: 1). Measurement of lightcurves and 2). Deep Learning. Hence, the literature study is further divided into 2 subsections.

A. Measurement of lightcurves based debris detection

In [24], Carolin Früh et al. conducted an analysis on light curves of space debris that are regularly examined using the 1-meter Zimmerwald Laser and Astrometric Telescope (ZIMLAT). The majority of the light curves discussed by the authors are captured from space debris items and are not in the official United States Strategic Command (USSTRATCOM) catalog for space debris, but are archived in the Astronomical Institute of the University of Bern's (AIUB) internal catalog. The approach followed by them to categorise unidentified objects and simplify things is to characterise known items. Light curves obtained with ZIMLAT have a sampling rate of about three seconds and it recorded the light curves of a defunct Gorizont 45L satellite. Gorizont 45L satellite was launched in July 2000 as one of the 35 Russian geosynchronous communications satellites of Gorizont constellation (launched between 1978 and 2000) to provide a satellite relay system for the 1980 Olympic Games in Moscow, eight years after being launched, the satellite's stabilisation mechanism ceased in March 2008, causing it to drift at a pace of 0.3° West each day. The Gorizont 45L satellite is a cylindrical body with two wider and a smaller solar panel. It is a space debris with no longer attitude controlled and there appears to be a pattern in each of the light spectrum measurements detected by ZIMLAT for this large satellite, which is believed to depict the panel-body structure.

In [25], Georg Kirchner et al. addressed the contribution of data from a Satellite Laser Ranging (SLR) station equipped with a Cassegrain receiver telescope of focal length 50 cm and a transmit telescope of focal length 10 cm parallel to it in Graz, Austria. The station consists of these telescopes as the only remaining components from the Graz SLR station's original configuration, which began monitoring space objects in lower earth orbit with a 10 Hz Nd:YAG laser in 1983. Since then, every component like computers, sensors, lasers, timing units, optical sensors etc. - has been routinely changed and modified. The data collected by the SLR station contributed in precise estimation of characteristics of space debris. The station works on identifying space debris targets containing retro-reflectors on them using laser ranging as well as space debris targets without containing retro-reflectors on them using single-photon light curve recording. The laser ranging technique is similar to that we have discussed in [24]. A single-photon light curve detecting system is also installed at the station in which solar photons diffusely reflected from objects are detected using a single-photon avalanche detector. These detections are recorded in a Field Programmable Gate Array (FPGA) throughout time periods that may be selected - typically between 10ms, thus providing a resolution of over 100 Hz. When the behaviour of target changes, so does the reflectivity, allowing the spin of the target to be recorded. Spin parameters can also be calculated through comprehensive investigation, for e.g., spin axis alignment and its variations. Moreover, it is practically possible to record the event time of each photon, resulting in a light curve with exceptionally high precision. When compared to charge-coupled device (CCD) imaging equipment, this approach produces substantially smaller data files and it is also intrinsically single-photon sensitive. The only drawback of this method is that the station must be in complete darkness and the targets must be in direct sunlight; for LEOs, this limits the termination period for light curve recordings to last roughly about two hours.

The period of spin is typically calculated using Phase Dispersion Minimization (PDM). All phases of each entire rotation are averaged and plotted, this produces exceptionally clear image data of a full phase of one rotation and provides precise spin duration estimates.

B. *Deep Learning based debris detection*

In [26], Tan Wu et al. developed a two-stage convolutional neural network (TSCNN) with locating and identification capabilities Further, to get better locating accuracy they used minimum bounding rectangle with threshold (MBRT). The dataset used here consisted of around 550 target models from a public database. Later the number of images were increased to 30440 by data augmentation methods such as rotation, transposition, inversion, snipping, adding noise, and combining with other images. Figure 2 shows some results of data augmentation.

A Network consisting two stages namely, locating module and recognition module is implemented. The first stage is intended to locate and slice the desired target region.

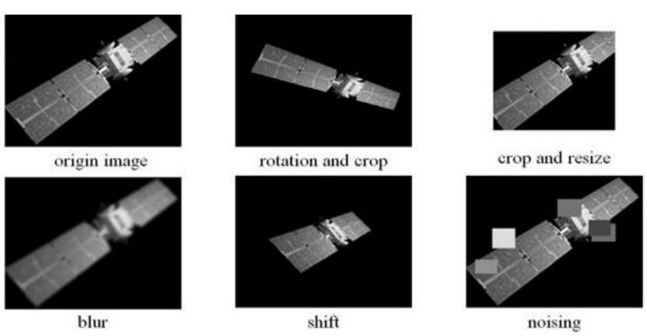

Fig. 2. Results from data augmentation [26]

To increase the finding speed, modified concept of MBRT is used. MBRT concept is also used for collection and clip off of the smallest rectangular sections containing suspicious targets as the simulated high-definition deep space image with a resolution of 2048x2048 pixels would take too long to analyse directly, then the sections are made and transmitted to the recognition network. In the second stage the proposal regions are sent to the ResNet-50 model which serves as a main pillar layer for attribute extraction, after which the trained predictor can sort the proposal areas. Figure 3 represents the architecture of ResNet-50 equipped with MBRT, since ResNet-50 model has a favourable consequence on relatively easier object identification, a deeper network is more likely to produce over-fitting.

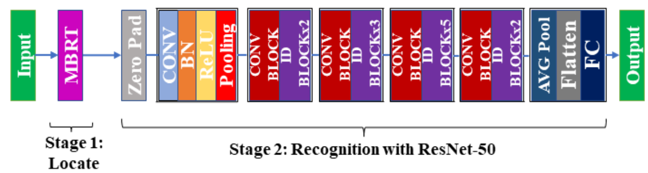

Fig. 3. The overall architecture of ResNet50 equipped with MBRT [26]

This technique achieved an overall accuracy of 99.94% and demonstrated an accurate assessment on one of the produced 2048x2048 deep space image containing four satellites.

In [27], Jiang Tao et al. introduced a DCNN for spatiotemporal saliency map based on FCN (Fully connected network). The FCN described here takes two frames from observer's video data as input, incorporates the local contrast data produced by the local contrast measure as prior of salient region and generates a finalized spatiotemporal saliency map directly. The model consists of a sequence of convolutional layers (CL) and deconvolutional layers. The frame pair and local contrast map denoted by (I_t, I_{t+1}) and P_t of I_t respectively, are combined in the channel path. As a result, a tensor with dimensions (h, w, 7) is fed into the FCN network, where h, w, 7 respectively corresponds to the height, breadth, and channel number of tensor. Every CL has Rectified Linear Units (ReLUs) behind it to enhance feature representation followed by max-polling layers. Various deconvolutional layers are placed below the CL to upsample the raw attribute map generated by CL and max pooling layers, as pixel-wise saliency prediction is more effective for saliency detection.

According to the authors, this CNN-based detection approach was proposed for the first time for small space debris detection. As a result, authors were unable to compare any relative methods except the existed CNN-based object recognition approach proposed by Wang W et al. in [28] and the results shows that it is effective for small space debris detection and has a good robustness at varying noise background.

In [29], Roya Afshar & Shuai Lu suggested training a CNN to categorise and estimate the pose of space debris at the same time, The dataset used here was BUAA-SID 1.0 and BUAA-SID 1.5 [30] consisting of 2 training-sets and 3 testing-sets. Transfer-learning mechanisms were adopted for faster training and better feature extraction, the limited size of BUAA-SID dataset is expanded using the Keras Data Generator Tool as an augmentation strategy to improve precision, the performance of the suggested architecture is analysed under various space environment situations, such as noisy and various illumination angles. The major issue here was to develop a robust visual representation that enables this model to categorise debris image and calculate the camera frame's orientation (C), by taking into account the target spacecraft's body frame (B), this can be achieved by taking the difference between reference of target object and the observer camera also known as the rotation matrix (R), as illustrated in Figure 4.

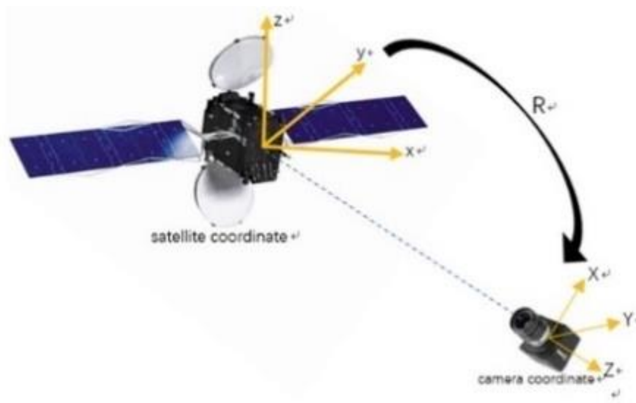

Fig. 4. Image representing satellite and camera coordinate system [29]

Prediction $\hat{t}$ of the above issue is described as follows:

$$\hat{t}_{\theta,W} = F_W \cdot z_\theta(x_i) \quad (1)$$

z_θ denotes how the input data x_i is transformed into the attribute, later the output layers of our model are fed with this data. F_W represents a set of output layer operation that involve taking the deep feature map $z_\theta(x_i)$ as input, following objective function is defined based on the prediction model in equation (1)

$$argmin_{\theta,W} \mathrm{L}(\theta, w) \quad (2)$$

Hence, the loss function with viewpoint estimation ($\emptyset$) and classification (y) follows equation (3)

$$\mathrm{L}(\theta, w) = \lambda_1 \mathrm{L}_y(\theta, W^y) + \lambda_2 \mathrm{L}_\emptyset(\theta, W^\emptyset) \quad (3)$$

During the training phase, the scalar variable λ determines the importance of a special loss. The pose estimation loss was traditionally considered from both continuous and discrete viewpoints, and a Categorical Cross-entropy function is employed for the classification loss, Moreover, pose estimation is treated as a classification issue in discrete formulations whereas it is addressed by regression in continuous formulations. Due to the coarse quantization of the dataset, Mean Squared Error was utilised in this study to address the regression problem.

In this architecture, the position estimation work is partially isolated from the satellite classification work. There are two stages for these two goals as shown in Figure 5, To extract the attributes, in the first phase, a pre-instructed network is utilised with hyper- parameters from the Image net dataset. In the second phase, network is trained for classification and regression, however, the pose regression and satellite identification branches are independent. By solving the objective function shown in Eq. (3), the model is trained. During the training processes λ_1=0 for pose route while, λ_2=0 for the detection route.

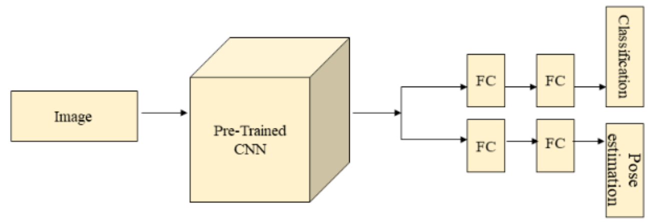

Fig. 5. Model representation of CNN architecture used for pose estimation. [29]

The network is trained by BUAA-SID dataset involving a group size of 32 training samples and after 20 epochs, reached an overall accuracy of 99.24%.

In [31], Richard Linares and Roberto Furfaro proposed a method in which brightness measurements derived from electrical-optical sensors is used to classify space debris. A layered hierarchical architecture is utilised to extract attributes from brightness measurements, based on a DCNN model, the DCNN architecture used here is shown in Figure 6.

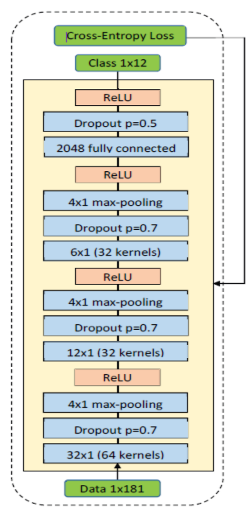

Fig. 6. Network architecture of brightness measurements based deep CNN model [31]

Simulated situations are used to illustrate the effectiveness of different space debris classification. Furthermore, physics-based models are used to generate the training samples that account for rotational dynamics and light reflection characteristics of space debris. The data set used here to train the model consists of light curve measurement vectors as inputs and class vectors as outputs. Then, using a collection of training samples, the DCNN with a fully connected output layer is trained to map from measurement vector to classes as shown in Figure 6. The number of convolution filters for each CL determines the number of output maps and each of these CL has a collection of kernels of a specific size that are learnt from the data.

The cross-entropy (CE) loss function was used as the cost function in this study. The CE loss between training outputs and CNN outputs is minimised using this cost function. The CNN classification technique is then trained using stochastic gradient descent by reducing the CE loss from the outputs compared to the labelled data. This approach reached an overall accuracy of 99.60% of correct classification when tested against 5000 data samples.

In [32], A. Montanaro et al. proposed a novel trigger algorithm that combines a stacking technique as well as a CNN, known as STACK-CNN. This technique can detect fragmentation debris orbiting at over 17,500 mph in earth's orbit, this method was initially designed as an offline apparatus for the International Space Station's Multiwavelength Imaging New Instrument for the Extreme Universe Space Observatory (Mini-EUSO) [33]. Its algorithm uses stacked images produced by overlapping of multiple frames. Depending on the relative velocity and direction of an object in a telescope's field of view, if the stacking method precisely matches the object's velocity and direction, then the resulting integrated picture is composed of a single brighter point at the object's starting position. However, a decision algorithm is required since the object's exact feature is not know in advance and the stacking method generates a large number of possibilities based on all potential configurations. Moreover, a trigger system consisting of a super-wide field-of-view telescope (EUSO) and a unique high-efficiency fibre-based laser system can be utilised to overcome this issue.

To investigate the efficacy of the Mini-EUSO detector in detecting the presence of space debris the authors used the EUSO Simulation and Analysis Framework (ESAF) [34]. The approach is then compared to a standard trigger technique established in the framework of cosmic ray science and modified for space debris, and the authors found that the STACK-CNN performs better.

In [35], Nouar Aldahoul, et al. proposed an approach that provides a multi-modal (MM) learning result using DL models. To take out information from Red-green-blue (RGB) channel image containing space objects including space debris, CNN models such as ResNet, EfficientNet [36], and DenseNet [37] are investigated. Additionally, an RGB image based visual transformer is introduced by the authors, the classification of depth images was done using End-to-End CNN (EECNN) [38] and the final decision of the solution is calculated by combining the two conclusions from RGB and Depth-based models. The Spacecraft Recognition leveraging Knowledge of space environment (SPARK) [39] dataset created in a realistic space simulation environment containing diverse pictures grouped into eleven categories is used. The goal of this method is to categorise orbital space objects into 11 categories namely, TRMM, Terra, Sentinel-6, Calipso, Debris, Jason, CloudSat, CubeSat, Aura, Aquarius, and AcrimSat. For challenges of machine translation, Vaswani et al. [40] introduced a DL model called vision transformer (VT). This transformer was modified to a VT for computer vision tasks involving image classification, where it was found to surpass the efficacy of some of the best CNN-based techniques in image recognition applications. Two models are introduced in this solution, the first one is VT pre-trained on the ImageNet 21 k dataset and fine-tuned on the ImageNet 2012 dataset, eleven categories were produced by tuning only the transformer's upper layers with RGB space images. The EECNN is used as the second model to learn the characteristics of depth images and map them into 11 categories.

This method was compared with several MM learning CNN techniques consisting only two models. DCNN such as ResNet50, DenseNet201, or EfficientNetB7 each pre-trained on ImageNet 2012 served as the first model, these pre-trained networks are then used for attribute extraction by freezing the backbone network and adding support vector machine (SVM) classifier in place of the top layers with images to create eleven categories, the second model used in these methods are identical to the second model of EECNN solution.

The various evaluation metrics, including accuracy, precision, recall, and F1-score are used to analyse the classification performance, as discussed below, followed by series of experiments.

1. Accuracy generally describes how the model performs across all classes.

$$\text{Accuracy} = \frac{tp+tn}{tp+fp+tn+fn} \quad (4)$$

2. Recall or Sensitivity is the Ratio of true positives to total (actual) positives in the data.

$$\text{Recall} = \frac{tp}{fn+tp} \quad (5)$$

3. Precision is the Ratio of true positives to total predicted positives.

$$\text{Precision} = \frac{tp}{tp+fp} \quad (6)$$

where tp: True Positive, tn: True Negative, fp: False Positive, fn: False Negative.

4. F1-score is the weighted average of Precision and Recall.

$$\text{F1-score} = \frac{2 \text{ x } precision \text{ x } recall}{precision + recall} \quad (7)$$

The first experiment was conducted to compare EECNN and a pre-trained DenseNet201 CNN + SVM model. The second experiment was carried with three pre-trained networks namely, ResNet50, EfficientNetB7, and DenseNet201 each combined with SVM, these networks are used for classifying RGB images containing space debris objects. Third experiment was conducted to analyse the performance of MM method, which combines VT utilising RGB images and EECNN utilising depth images. The fourth and final experiment examines MM learning with single-modal learning including, single DenseNet201 CNN, single EfficientNetB7 CNN, single ResNet-50 CNN each combined with SVM and single Vision Transformer. From the experiments, the accuracy of the above algorithms are as follows:

TABLE II. ACCURACY COMPARISION FOR VARIOUS TECHNIQUES TRAINED WITH SPARK DATASET [35]

Algorithm	Accuracy (%)	Recall (%)	Precision (%)	F1 score
DenseNet201- Depth	68	67	68	0.68
EECNN- Depth	70	70	69	0.69
ResNet50 CNN- RGB	72	70	76	0.69
EfficientNetB7 CNN—RGB	80	78	81	0.76
DenseNet201 CNN—RGB	74	72	77	0.70
VT—RGB	81	80	83	0.78
MM (ResNet50 and EECNN)	80	79	81	0.79
MM (EfficientNetB7 and EECNN)	85	84	85	0.83
MM (DenseNet201 and EECNN)	81	80	82	0.80
MM (VT and EECNN)	85	85	86	0.84

From the above results it can be noted that, compared with other techniques discussed by the author, the MM (Vision Transformer and EECNN) gives better accuracy, recall, precision and F1-score.

In [41], Haoyue Zeng, et al. proposed a nine-layered DCNN model to perform space debris identification. Furthermore, to mimic the true imaging conditions in space, a simulated space target dataset was employed, with pictures generated by a space satellite simulation software called the Systems Tool Kit (STK) [42] and degraded by a series of motion blur and out-of-focus blur. There were four target classes in this dataset, each with 100 images. The DCNN model utilised here is built using the LeNet-5 [43] architecture as a foundation. This DCNN has nine layers, comprising three CLs, three spatial pooling layers, and three fully linked layers, as illustrated in Figure 7.

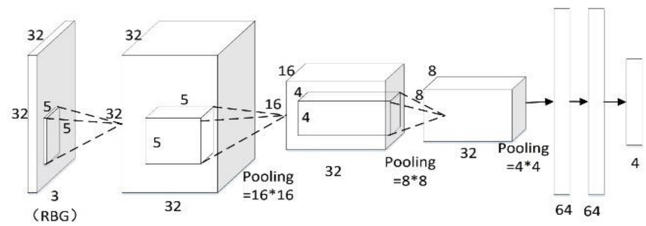

Fig. 7. Architecture of nine-layer CNN [41]

By artificially increasing the training dataset, data augmentation can reduce the over-fitting of DCNN models. Furthermore, label preserving transformations such as rotation, transposition, inversion, snipping, homography and noise injection is used to create augmented pictures for each image. With the simulated STK dataset consisting of 24- fold training data and 12-fold testing data, the authors compared this approach with several existing approaches and concluded that this deep learning approach has demonstrated promising results when compared to traditional shallow learning methods.

III. OVERVIEW OF METHODS OF CLASSIFICATION

Table 3, summarises the space debris detection methods, quality of the results and validate the conclusions based on the results. It shows the comparability of above methods based on Techniques used, accuracy, advantages and their limitations.

TABLE III. METHODS FOR CLASSIFYING SPACE DEBRIS USING CNN THAT HAVE BEEN USED IN PRIOR RESEARCH ARTICLES

References and Year	**Technique**	**Accuracy**	**Advantages**	**Limitations**
[26], 2019	TSCNN with MBRT and ResNet-50	99.94%	MBR concept is also used for collection and clip off of the smallest rectangular sections containing suspicious targets.	Too much data augmentation can result in overfitting
[29], 2020	TSCNN trained with hyper-parameter of Image-net dataset.	99.24%	Categorise and estimate the pose of space debris simultaneously.	Since the calculations are based on a simulated dataset, they may deviate from real-world scenario.
[27], 2019	FCN based spatiotemporal saliency platform.	_	ReLUs used to enhance feature representation followed by max-polling layers	For training, a huge dataset is necessary, as well as a high computing cost.
[31], 2016	CNN based on brightness measurements	99.60%	simpler implementation	Computationally expensive
[32], 2022	STACK-CNN	_	Can detect high velocity fragmentation debris.	Stacking method generates a large number of possibilities.
[35], 2022	Multi-modal (Vision Transformer and End-to-End CNN)	85%	Can reach high accuracy with large dataset	Highly complex network
[41], 2017	9-layer DCNN	99.90%	Can identify required parameters accurately.	Model is trained using simulated dataset which may deviate from the real scenarios.

IV. CONCLUSIONS

This paper summarises the broad state-of-the art for the approaches to detect and classify space debris. Detecting space debris in satellite images has recently become an important research issue in computer vision. In many computer vision applications, analyzing noisy and low-resolution images is a major challenge. There are various remote inspection methods available for space debris identification, but the aim of this analysis is on satellite image-based methods. Some light curve measuring methodologies are investigated utilising the 1-meter Zimmerwald Laser and Astrometric Telescope (ZIMLAT) and several image-based space debris detection models were evaluated and reviewed using various image datasets in this survey. DL algorithms like TSCNN, FCN and CNN are used to classify space debris. Performances are analysed for space debris classification based on accuracy, recall, F1-score, and precision, although the existing methods yield outstanding results, with the majority of them already being implemented, Space debris detection still need improvement. DL has significantly enhanced the performance of Space debris detection algorithms.

As part of future research, the authors can explore new ways to train models by non-simulated training datasets to enhance the precision of space debris detection. The study reported in this paper will undoubtedly aid future researchers engaged in merging DL with space debris detection and management.

V. REFERENCES

[1] Kessler, Donald J., and Burton G. Cour-Palais. "Collision frequency of artificial satellites: The creation of a debris belt." *Journal of Geophysical Research: Space Physics* 83, no. A6 (1978): 2637-2646.

[2] Klinkrad, Heiner. Space debris: models and risk analysis. *Springer Science & Business Media*, 2006.

[3] Smirnov, Nickolay N. Space Debris: Hazard Evaluation and Debris. *CRC Press*, 2001.

[4] Zhang, Yizhe, Xin Guan, Xian Zhao, and Lei Liu. "Ground Experiment development for acquiring, tracking and pointing of small space debris." *The Journal of the Astronautical Sciences* 66, no. 1 (2019): 68-82.

[5] H. Klinkrad, et al. The ESA Space Debris Mitigation Handbook 2002. *Advances in Space Research*, January 2004, 34(5):1251–1259.

[6] Shan, Minghe, Jian Guo, and Eberhard Gill. "Review and comparison of active space debris capturing and removal methods." *Progress in Aerospace Sciences* 80 (2016): 18-32.

[7] Ntumba, Manuel, and Saurabh Gore. "Avancee-1 Mission and SaDoD Method: LiDAR-based stimulated atomic disintegration of space debris (SaDoD) using Optical Neural Networks." *arXiv preprint arXiv:2105.13485* (2021).

[8] Li, Shuang, Ruikun Lu, Liu Zhang, and Yuming Peng. "Image processing algorithms for deep-space autonomous optical navigation." *The Journal of Navigation* 66, no. 4 (2013): 605-623.

[9] Khan, Mohd Aijaj, and Manish Dixit. "Discovering Exoplanets in Deep Space using Deep Learning Algorithms." In *2020 12th International Conference on Computational Intelligence and Communication Networks (CICN)*, pp. 441-447. IEEE, 2020.

[10] González, Roberto E., et al. "Galaxy detection and identification using deep learning and data augmentation." *Astronomy and computing* 25 (2018): 103-109.

[11] Joseph, S. "Accurate Segmentation for Low Resolution Satellite images by Discriminative Generative Adversarial Network for Identifying Agriculture Fields." *Journal: Journal of Innovative Image Processing December* 2021, no. 4 (2021): 298-310.

[12] Khalil, Mahmoud, Elena Fantino, and Panos Liatsis. "Evaluation of Oversampling Strategies in Machine Learning for Space Debris Detection." In *2019 IEEE International Conference on Imaging Systems and Techniques (IST)*, pp. 1-6. IEEE, 2019.

[13] National Research Council. *Limiting future collision risk to spacecraft: an assessment of NASA's meteoroid and orbital debris programs*. National Academies Press, 2011.

[14] Yao, L. U., and Z. H. A. O. Chang-yin. "The Basic Shape Classification of Space Debris with Light Curves." *Chinese Astronomy and Astrophysics* 45, no. 2 (2021): 190-208.

[15] Allworth, James, et. al. "A transfer learning approach to space debris classification using observational light curve data." *Acta Astronautica* 181 (2021): 301-315.

[16] Zeng, Haoyue, and Yong Xia. "Space target recognition based on deep learning." In *2017 20th International Conference on Information Fusion (Fusion)*, pp. 1-5. IEEE, 2017.

[17] Gupta, P., Dixit, M. Image-based crack detection approaches: a comprehensive survey. *Multimed Tools Appl* (2022). https://doi.org/10.1007/s11042-022-13152-z

[18] Krizhevsky, Alex, Ilya Sutskever, and Geoffrey E. Hinton. "Imagenet classification with deep convolutional neural networks." *Advances in neural information processing systems* 25 (2012).

[19] Simonyan, Karen, and Andrew Zisserman. "Very deep convolutional networks for large-scale image recognition." *arXiv preprint arXiv:1409.1556* (2014).

[20] Szegedy, Christian, et al. "Going deeper with convolutions." In *Proceedings of the IEEE conference on computer vision and pattern recognition*, pp. 1-9. 2015.

[21] He, Kaiming, et al. "Deep residual learning for image recognition." In *Proceedings of the IEEE conference on computer vision and pattern recognition*, pp. 770-778. 2016.

[22] Chen, Zhang, and Zhao Changyin. "Activities of PMO optical space debris survey." *Anais da Academia Brasileira de Ciências* 93 (2021).

[23] Jahirabadkar, Sunita, et al. "Space objects classification techniques: A survey." *In 2020 International Conference on Computational Performance Evaluation (ComPE),* pp. 786-791. IEEE, 2020.

[24] Fruh, Carolin, and Thomas Schildknecht. "Analysis of observed and simulated light curves of space debris." In *Proceedings of the international Astronautical Congress*. 2010.

[25] Kirchner, Georg, et al. "Determination of attitude and attitude motion of space debris, using laser ranging and single-photon light curve data." In *Proceedings of the 7th European Conference on Space Debris, Darmstadt, Germany*, pp. 18-21. 2017.

[26] Wu, Tan, et al. "T-SCNN: A two-stage convolutional neural network for space target recognition." In *IGARSS 2019-2019 IEEE International Geoscience and Remote Sensing Symposium*, pp. 1334-1337. IEEE, 2019.

[27] Tao, Jiang, et al. "Deep Convolutional Neural Network Based Small Space Debris Saliency Detection." In *2019 25th International Conference on Automation and Computing (ICAC)*, pp. 1-6. IEEE, 2019.

[28] Wang, Wenguan, Jianbing Shen, and Ling Shao. "Video salient object detection via fully convolutional networks." *IEEE Transactions on Image Processing* 27, no. 1 (2017): 38-49.

[29] Afshar, Roya, and Shuai Lu. "Classification and Recognition of Space Debris and Its Pose Estimation Based on Deep Learning of CNNs." In *International Conference on Human-Computer Interaction*, pp. 605-613. Springer, Cham, 2020.

[30] Zhang, H., Z. Liu, Z. Jiang, M. An, and D. Zhao. "BUAA-SID1. 0 space object image dataset." *Spacecraft Recovery & Remote Sensing* 31, no. 4 (2010): 65-71.

[31] Linares, Richard, and Roberto Furfaro. "Space object classification using deep convolutional neural networks." In *2016 19th International Conference on Information Fusion (FUSION)*, pp. 1140-1146. IEEE, 2016.

[32] Montanaro, A., T. Ebisuzaki, and M. Bertaina. "Stack-CNN algorithm: A new approach for the detection of space objects." *Journal of Space Safety Engineering* 9, no. 1 (2022): 72-82.

[33] Casolino, M., et al. "The Mini-EUSO telescope on board the International Space Station: Launch and first results." *arXiv preprint arXiv:2201.01213* (2022).

[34] Thea, A., et al. "The EUSO simulation and analysis framework." In *29th International Cosmic Ray Conference (ICRC 2005)*, pp. 133-136. 2005..

[35] AlDahoul, Nouar, Hezerul Abdul Karim, and Mhd Adel Momo. "RGB-D based multi-modal deep learning for spacecraft and debris recognition." *Scientific Reports* 12, no. 1 (2022): 1-18.

[36] Tan, Mingxing, and Quoc Le. "Efficientnet: Rethinking model scaling for convolutional neural networks." In *International conference on machine learning*, pp. 6105-6114. PMLR, 2019.

[37] Huang, Gao, et al. "Densely connected convolutional networks." In *Proceedings of the IEEE conference on computer vision and pattern recognition*, pp. 4700-4708. 2017.

[38] Glasmachers, Tobias. "Limits of end-to-end learning." In *Asian conference on machine learning*, pp. 17-32. PMLR, 2017.

[39] Musallam, Mohamed Adel, et al. "SPARK: spacecraft recognition leveraging knowledge of space environment." *arXiv preprint arXiv:2104.05978* (2021).

[40] Vaswani, Ashish, et al. "Attention is all you need." *Advances in neural information processing systems* 30 (2017).

[41] Zeng, Haoyue, and Yong Xia. "Space target recognition based on deep learning." In *2017 20th International Conference on Information Fusion (Fusion)*, pp. 1-5. IEEE, 2017.

[42] Zhang, W., et al, 2013, July. Optical image simulation system for space surveillance. In *2013 Seventh International Conference on Image and Graphics* (pp. 721-726). IEEE.

[43] LeCun, Yann, et al. "Gradient-based learning applied to document recognition." *Proceedings of the IEEE* 86, no. 11 (1998): 2278-2324.